IEEE Access
Multidisciplinary : Rapid Review : Open Access Journal

Received April 27, 2018, accepted May 26, 2018, date of publication June 4, 2018, date of current version June 26, 2018.

Digital Object Identifier 10.1109/ACCESS.2018.2843795

A High-Transmittance Frequency-Selective Rasorber Based on Dipole Arrays

ZHEFEI WANG[1], QINGSHENG ZENG[2], (Senior Member, IEEE), JIAHUI FU[1], (Senior Member, IEEE), WAN CHEN[1], BO LV[1], MINGXIN SONG[3], AND TAYEB A. DENIDNI[4], (Senior Member, IEEE)

[1]School of Electronics and Information Engineering, Harbin Institute of Technology, Harbin 150001, China
[2]College of Astronautics, Nanjing University of Aeronautics and Astronautics, Nanjing 210016, China
[3]College of Applied Science, Harbin University of Science and Technology, Harbin 150001, China
[4]Institut National de la Recherche Scientifique, Université du Quebec, Montreal, QC H5A1K6, Canada

Corresponding author: Jiahui Fu (fjh@hit.edu.cn)

This work was supported in part by the National Natural Science Foundation of China under Grant 61571155 and in part by the Aeronautical Science Foundation of China under Grant 20151877001.

ABSTRACT This paper presents a frequency-selective rasorber whose transmission window locates at the higher frequency of absorption band. The accomplished rasorber is composed of dipole-like and slot arrays, and has realized the transmissive/absorptive performance. In every unit cell, each pair of dipole-like elements connected by vias is printed on the two sides of the substrate, and the coupling between long and short dipoles is suppressed by this structure. A guiding circuit is studied based on the analysis of the current path, and the insertion loss of transmission window is significantly reduced by the surface current at the pass-band that is hindered to pass through lossy elements. The presented rasorber acts as an absorber at the low frequencies, while providing a high transmittance window at 5.6 GHz. This design is elaborately optimized to achieve low reflection and angle-insensitive performance. Finally, the presented structure is validated by numerical simulations and experimental measurements. This rasorber could be used for secrecy communications among stealth facilities while providing stable broad-band absorptive properties.

INDEX TERMS Absorption, frequency-selective rasorber, high transmittance, low reflection.

I. INTRODUCTION

A stealth system plays a crucial role in the competition of military industry. In the past, outstanding frequency selective and spatial filtering characteristics of frequency selective surfaces (FSS) have attracted a lot of interest of researchers [1]–[2], and have been utilized to avoid the potential threat from a hostile radar [3]–[5]. The detection power is reflected to other directions and would not influence the communication performance. As the development of detective radar system, the power reflected to other directions could be detected by a multistatic radar system. By inserting lossy elements and adding a reflection layer, an FSS can be structured as a frequency-selective absorber (FSA) [6]–[9]. An FSA features high absorptivity, so that less power is reflected within its operation band. However, the communication ability is limited by the covering FSA, and for that reason, frequency-selective rasorbers (FSR) with good absorptive/transmissive performance have extensively been studied in recent years [10].

The difficulty is that the high insertion loss caused by a lossy FSA cannot be eliminated simply by removing the backed reflection layer, since the power is consumed by the lossy elements. The low-pass characteristic of strip-type FSS has been used to constitute a rasorber in some recent designs [11]–[15]. By combining with the band-pass slot-type FSS, a transmission window is realized in low frequencies and the operation characteristic at the frequencies above the pass-band is similar to that of an absorber. Furthermore, several rasorbers whose pass-band locates at the frequencies above the absorption band have been proposed [16]–[17]. Other structures in [18]–[19] have allowed the incident power of higher frequency to pass by using distributed inductive and capacitive (*LC*) elements. A band-pass rasorber has been realized by using series lumped reactance elements in [20]. The incident wave out of the pass-band is absorbed, while the reflection over the whole operation band is reduced. Rasorbers composed of 3-D unit cell have been suggested in [21] and [22], the transmission band is expanded in these designs, while the wide-band absorptive performance cannot be provided at the same time. Few works realized a transmission window which locates at the frequencies above the stop-band in all of the designs above. For designs featuring a transmission window at high frequencies, the absorption band at low frequencies is relatively narrow, or strong reflection is introduced between the pass-band and stop-band.

The aim of this work is to design a new rasorber with a high transmittance window whose frequencies locate above the absorption band. The reflection within the operation band should be reduced while absorbing wide-band incident power. Based on our recent work [23], the precondition of absorptive/transmissive performance is studied using the *ABCD* and |S| matrices. A guiding circuit is presented in order to realize the desired performance. Generally, for most rasorbers, the transmission window is generated by *LC* elements. Different from the previous designs, a new lossy array is presented and designed to form the rasorber. This array is constituted by two pairs of dipole-like elements. For that reason, the complexity and cost of fabrication could be reduced, while introducing few uncertainty factors caused by lumped reactance elements. Meanwhile, the transmission window with low insertion loss is realized with 0°-45° incidence. Furthermore, the presented structure is validated by simulated and experimental results.

II. EQUIVALENT CIRCUIT ANALYSIS

The profile view of a rasorber structure is illustrated in Fig. 1. Generally, the rasorber is composed of lossy and lossless layers, which are connected by a spacer with thickness t. A rasorber should function as an absorber at the stop-band, and be transparent at the transmission band. The low reflection over the operation band is realized to achieve stealth performance. Two periodical FSSs can be equivalent to branch circuits, and cascade with a transmission line which is the equivalent circuit of the spacer. The impedance of the lossy layer and lossless layer is expressed by Z_a and Z_b, respectively. Z_0 and Z_1 denote the characteristic impedance of the open space and the spacer, respectively. According to the above discussion, the *ABCD* matrix of the network can be written as [20]:

$$\begin{bmatrix} A & B \\ C & D \end{bmatrix} = \begin{bmatrix} 1 & 0 \\ 1/Z_a & 1 \end{bmatrix} \begin{bmatrix} \cos\beta t & jZ_1 \sin\beta t \\ j(1/Z_1)\sin\beta t & \cos\beta t \end{bmatrix} \begin{bmatrix} 1 & 0 \\ 1/Z_b & 1 \end{bmatrix} = \begin{bmatrix} j\dfrac{Z_1}{Z_b}\sin\beta t + \cos\beta t & jZ_1\sin\beta t \\ j\dfrac{Z_1^2 + Z_aZ_b}{Z_1Z_aZ_b}\sin\beta t + \dfrac{Z_a+Z_b}{Z_aZ_b}\cos\beta t & j\dfrac{Z_1}{Z_b}\sin\beta t + \cos\beta t \end{bmatrix} \tag{1}$$

where $\beta = 2\pi/\lambda_0$, and λ_0 is the wavelength of open space. Generally, the value of Z_1 is selected same as Z_0 for a

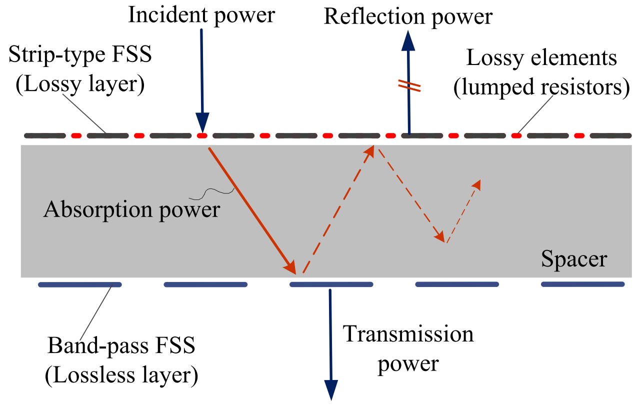

FIGURE 1. Side-view of a rasorber structure.

simplified calculation purpose. The expressions of $|S_{21}|$ and $|S_{11}|$ could be obtained through the *ABCD* matrix and are expressed as follows [24]:

$$|S_{21}| = \left|\frac{2}{A + B/Z_0 + CZ_0 + D}\right| = \left|\frac{2}{j(\frac{Z_0(Z_a+Z_b+Z_0)}{Z_aZ_b} + 2)\sin\beta t + (\frac{Z_0(Z_a+Z_b)}{Z_aZ_b} + 2)\cos\beta t}\right| \tag{2}$$

$$|S_{11}| = \left|\frac{A + B/Z_0 - CZ_0 - D}{A + B/Z_0 + CZ_0 + D}\right| = \left|\frac{j(\frac{Z_0(Z_a-Z_b-Z_0)}{Z_aZ_b})\sin\beta t - (\frac{Z_0(Z_a+Z_b)}{Z_aZ_b})\cos\beta t}{j(\frac{Z_0(Z_a+Z_b+Z_0)}{Z_aZ_b} + 2)\sin\beta t + (\frac{Z_0(Z_a+Z_b)}{Z_aZ_b} + 2)\cos\beta t}\right| \tag{3}$$

At the transmission band, $|S_{21}| = 1$. Based on (2), it can be seen that the values of Z_a and Z_b should be infinite. When the circuit operates at the stop-band, $|S_{21}|$ and $|S_{11}|$ should be zero. According to (2), $Z_a \times Z_b$ is equal to zero. It is obvious that Z_a is a complex number with ohmic loss and could not be zero. $Z_b = 0$ is taken as the solution at the stop-band and is substituted into (3), the following equation is obtained

$$|S_{11}|\,|_{Z_b=0} = \left|\frac{jZ_0(Z_a - Z_0)\sin\beta t - Z_0Z_a\cos\beta t}{jZ_0(Z_a + Z_0)\sin\beta t + Z_0Z_a\cos\beta t}\right| \xrightarrow{Z_a=Z_0,\,\beta t=\pi/4} |S_{11}|\big|_{Z_b} = 0 \tag{4}$$

Therefore, to satisfy the absorption condition, the lossless layer should function as a short circuit at the absorption band. A spacer with 1/4 wavelength of absorption frequency thickness should be adopted, and the real part of Z_a should be close to Z_0.

The presented rasorber should satisfy the constraint conditions discussed above. Moreover, for the reported designs whose transmission window located at the higher frequency of absorption band, the lumped resistors are used as lossy elements to fulfill the absorptive behavior. The transmission coefficient could be influenced due to the surface current

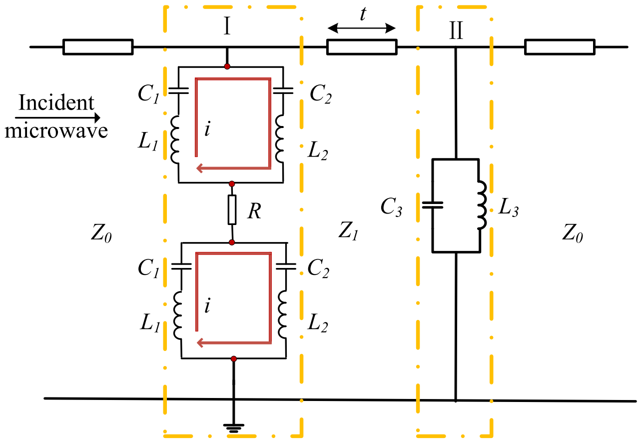

FIGURE 2. **Guiding circuit model of the presented rasorber.**

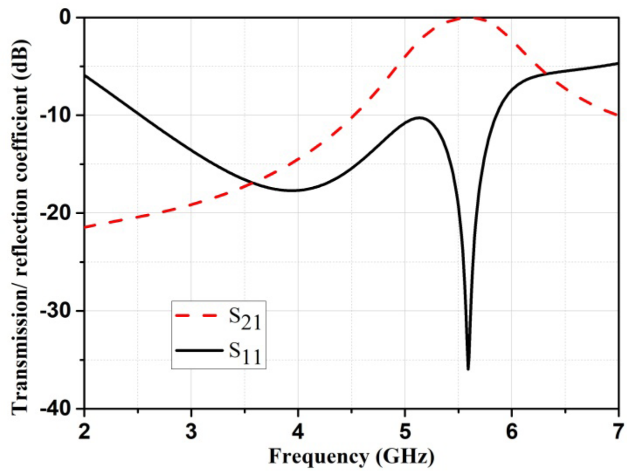

FIGURE 3. **Transmissive and absorptive performance of the guiding circuit.**

flowing through the lumped resistors. Therefore, the primary goal of this work is to realize infinite impedance of the lossy layer at the pass-band and reduce the current across the lumped resistors. To realize this goal, a guiding circuit model is studied and shown in Fig. 2. The presented circuit consists of two parts, named as I and II, and connected by a transmission line with the length of t. The parallel resonance can provide an infinite impedance for FSS structures. In part I, two pairs of identical parallel circuits (L_1, C_1 and L_2, C_2; $L_1 \times C_1 > L_2 \times C_2$) placed at the different sides of the resistor to guarantee the resistor is shielded at the pass-band. When the parallel circuits of part I work at the parallel resonance frequency (f_1), the current (i) is blocked in L_1, C_1 and L_2, C_2; therefore, the current through the branch nodes (four red dots in part I) is greatly reduced. Hence, the current through the resistor is significantly reduced at f_1, and a small insertion loss is introduced within the transmission band. Part II is a parallel branch circuit (L_3 and C_3) which functions as a band-pass filter characterized by a wide reflection band. The impedance of part II is zero and infinite at the stop-band and pass-band, respectively. Part I provides an ohmic loss (R) to achieve an absorptive performance with the lossless layer at the stop-band, and generates a transmission window at the same time. The part II should be resonant at f_1 in order to enable the incident power to pass through with small insertion loss. This circuit is transparent at f_1 since part I and II are open circuits and the characteristic impedance Z_1 is same as Z_0.

On the contrary, when the series circuits (L_1, C_1 or L_2, C_2) operate at the series resonance frequency (f_2 or f_3; $f_2 < f_3$), L_1, C_1 or L_2, C_2 can be equivalent to a shorted circuit. Since the part II presents a reflection feature except around f_1, the circuit operates as an absorber if an appropriate resistance value is selected. However, it is very difficult to use one resistance value to enable the circuit to match the characteristic impedance of free space at two resonance frequencies. Based on the goal of this work, the absorption band around f_3 is abandoned to realize an absorption band which locates below the pass-band. The resonance frequencies f_1, f_2 and f_3 satisfy the following relations:

$$\frac{[-j\frac{1-(2\pi f_1)^2L_1C_1}{2\pi f_1C_1}]\cdot[-j\frac{1-(2\pi f_1)^2L_2C_2}{2\pi f_1C_2}]}{[-j\frac{1-(2\pi f_1)^2L_1C_1}{2\pi f_1C_1}]+[-j\frac{1-(2\pi f_1)^2L_2C_2}{2\pi f_1C_2}]} = -j\frac{\left[1-(2\pi f_1)^2L_1C_1\right]\cdot\left[1-(2\pi f_1)^2L_2C_2\right]}{(2\pi f_1)\left[C_1+C_2-(2\pi f_1)^2L_1C_1C_2-(2\pi f_1)^2L_2C_1C_2\right]}=0 \quad (5)$$

$$j\frac{2\pi f_1L_3}{1-(2\pi f_1)^2L_3C_3}=0 \quad (6)$$

$$j\frac{1-(2\pi f_2)^2L_1C_1}{2\pi f_2C_1}=0 \quad (7)$$

$$j\frac{1-(2\pi f_3)^2L_2C_2}{2\pi f_3C_2}=0 \quad (8)$$

The estimated values of LC elements are obtained by employing the method proposed in [11] and [25]–[28]. It is worth pointing out that the simplest strip and slot FSSs are used to estimate the values of the series circuits (L_1, C_1 or L_2, C_2) and parallel circuit (L_3, C_3). To obtain the desired rasorber performance, we have optimized the estimated circuit element values by using the Tune Parameters Function of Advanced Design System (ADS). Finally, the circuit design has been conducted with following optimized values: $C_1 = 0.220$ pF, $L_1 = 8.34$ nH, $C_2 = 0.106$ pF, $L_2 = 2.82$ nH,$C_3 = 0.642$ pF, $L_3 = 1.269$ nH, $R = 500\ \Omega$, $Z_0 = Z_1 = 377$, and $h = 17.3$ mm. The simulated reflection and transmission coefficients of the presented circuit are shown in Fig. 3. It is seen that the desired performance of the rasorber is realized by this circuit. The transmission window locates at 5.6 GHz with a small insertion loss of 0.006 dB. Meanwhile, a stop-band is obtained from 2.5 GHz to 4.5 GHz with the reflection lower than −10 dB from 2.5 GHz to 5.8 GHz. At the frequencies above 5.8 GHz, the reflection increases gradually since the value of the resistor is optimized to obtain good absorptive performance around 3.5 GHz.

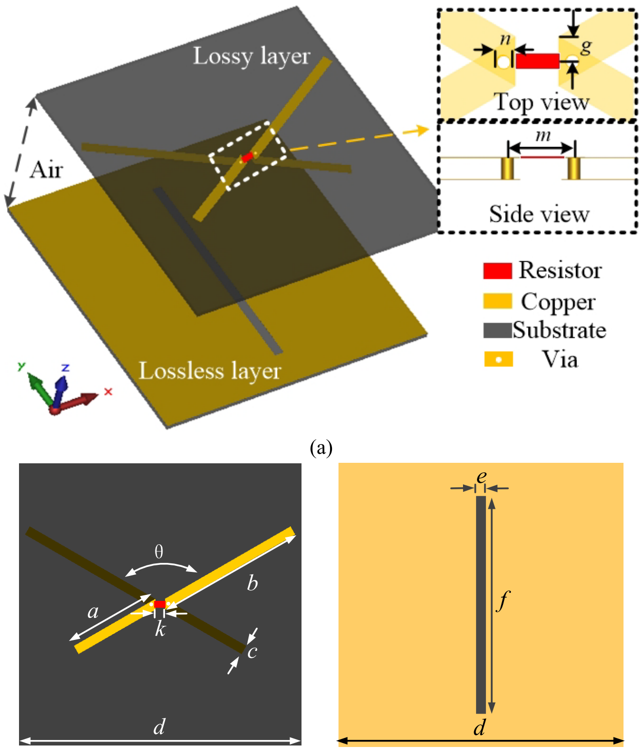

FIGURE 4. Unit cells of the presented rasorber. (a) Perspective view of the presented rasorber. (b) Top view of the lossy crossed dipole FSS unit cell. (c) Top view of the lossless slot FSS unit cell.

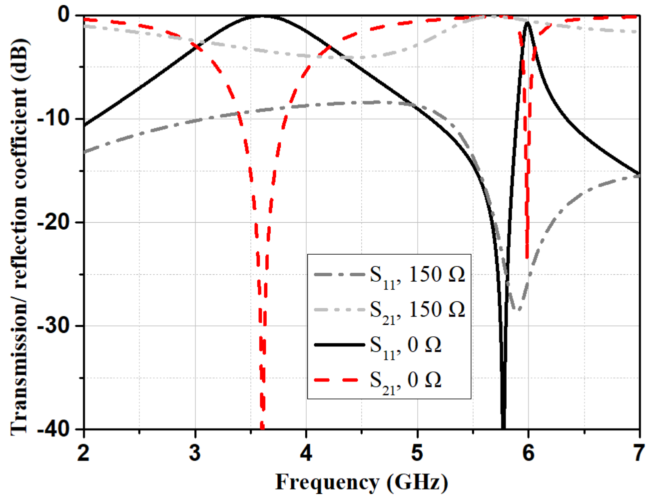

FIGURE 5. Simulated reflection and transmission results of the lossy layer with 0 Ω and 150Ω resistors.

III. IMPLEMENTATION OF THE RASORBER

The presented equivalent circuit can be obtained by periodical FSSs. The slot-type FSSs are used here to fulfill the band-pass circuit in part II, and the strip-type FSSs can provide series resonances. The transmission line between part I and II are realized by the air spacer. The geometry of a unit cell of the presented rasorber is illustrated in Fig. 4. The unit cell is periodic along x- and y-axes, where -z-axis is the direction of incidence. This structure is illuminated by the TM-polarized wave, whose electric-field directed along the x-axis. For the presented design, the thickness of substrates which support both lossy and lossless FSSs is 0.508 mm, and this parameter is chosen by taking both two side copper layers into account. The relative permittivity of the substrate is 2.2, and the distance between two FSS layers is 16 mm. Since two series *LC* circuits are connected to one side of the resistor, a rotated dipole-like element is selected to overcome the restriction of the physical structure.

The coupling between the connected neighboring long and short dipoles is very strong, so that two pairs of dipoles are placed on the different sides of the lossy layer, and vias are used to conduct the current between both sides. A resistor with 150 Ω is inserted into the gap of dipoles at the front side to connect two pairs of dipoles, meanwhile the gap of the back side is opened. Conversely, the lossless layer is realized by the one-side slot FSS. The equivalent inductance and capacitance values of the strip-type FSS can be determined from its physical dimensions and the distance between neighboring strip-type FSS, respectively. It is well known that the inductance shows a positive variation tendency with the total length of the dipole, and the capacitance is negatively related to the distance between two neighboring dipoles. Therefore, the long and short dipoles provide resonances at low and high frequencies, respectively. The physical dimensions of unit cells are chosen as follows: $a = 10$ mm, $b = 16$ mm, $c = 1$mm, $d = 30$ mm, $e = 1$mm, $f = 23$ mm, $g = 0.6$mm, $k = 1$ mm, $m = 1.6$ mm, $n = 0.3$mm and $\theta = 120°$

IV. SIMULATED AND EXPERIMENTAL RESULT ANALYSIS

The performance of the designed rasorber is analyzed with a commercial electromagnetic simulation software: CST Microwave Studio. The transmission and reflection results of the lossy layer are plotted in Fig. 5. The lossy FSS serves as a band-stop filter with a resistor of 0 Ω inserted which resonates at 3.6 GHz and 6 GHz. By inserting a resistor of 150 Ω, the quality factor in the stop-bands drops sharply due to the ohmic loss. Nevertheless, the transmission coefficient around the pass-band is almost not influenced, and it provides a potential possibility to realize a transmission window at that frequency. For the lossless FSS layer, it should be optimized to resonate between 5.4 GHz to 5.8 GHz to generate a pass-band.

The joint simulation results of lossy and lossless FSSs are shown in Fig. 6, and the performance under the oblique incidence is explored. As expected, a transmission band is realized at 5.6 GHz with 0.2 dB insertion loss under normal incidence. From 2.8 GHz to 5.7 GHz the reflection is under −10 dB with a fractional bandwidth of 68%, and a low radar cross section (RCS) performance is realized. The absorption band is over 2.8 GHz to 5 GHz, meanwhile there is no harmonic resonance introduced during the operation band. For oblique incidence, the absorptive performance is almost

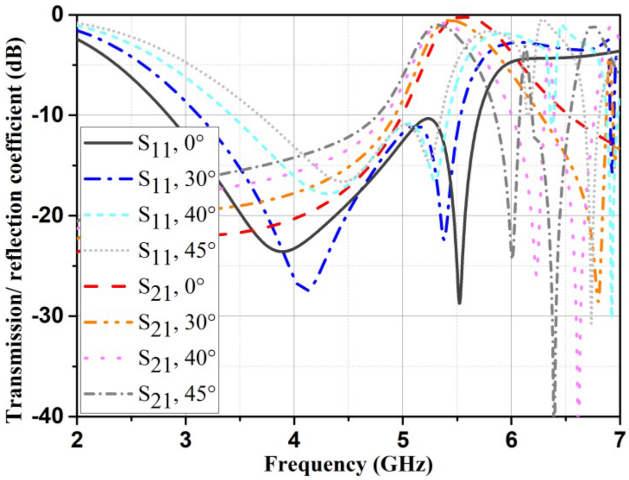

FIGURE 6. Simulated results of the presented rasorber under the oblique incidence.

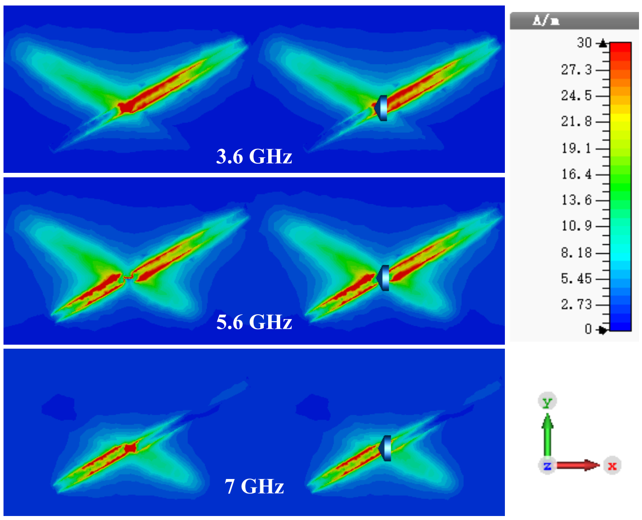

FIGURE 7. The surface current distribution on crossed dipoles with resistors at 3.6 GHz, 5.6 GHz and 7 GHz.

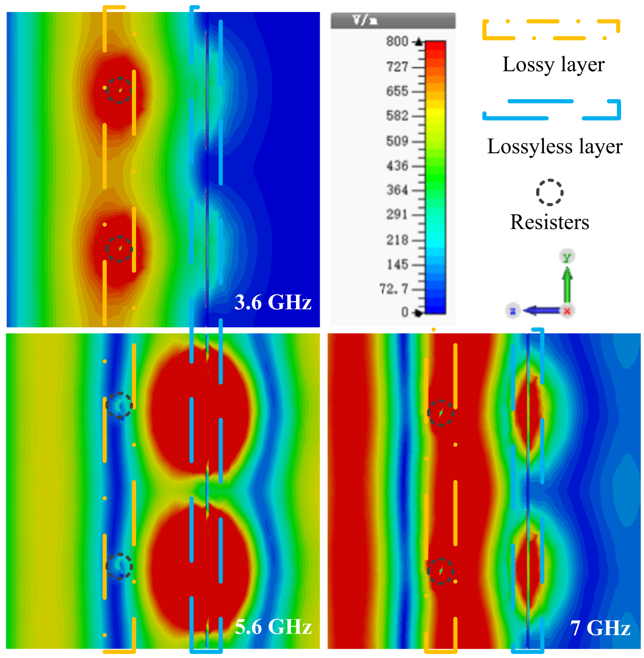

FIGURE 8. The electric-field distribution on the plane of the propagation direction of the incident wave at 3.6 GHz, 5.6 GHz and 7 GHz.

not affected up to 30° and starts to deteriorate after 40°. It is because that the length of the transmission line that is the equivalent circuit of the spacer is sensitive to the oblique incidence, and the input impedance of rasorber is changed under the oblique incidence. However, the reflection between the absorption band and transmission band is below -10 dB under 0°-45° incidence. Furthermore, the maximum insertion loss is less than 1 dB under 45° incidence, which could be deemed as a good behavior under the oblique incidence. The transmission peak is slightly shifted towards lower frequencies as the incidence angle increases, since the electrical length is increased under the oblique incidence.

Next, the surface current and electric-field distributions of the rasorber are investigated to verify the presented concept. The surface current of dipoles excited by the impinging electric-field is shown in Fig. 7. The lumped resistors of the left dipoles are hidden for observing the current between the dipoles more clearly. The long dipoles resonate at 3.6 GHz and then there is strong current excited on two long dipoles. The current density flowing across the resistor is so high that most of the incident power is consumed by resistors. At 5.6 GHz, the current through the cascaded resistor is very low even though both long and short dipoles are resonant. The current is blocked in four dipoles, and thus a transmission window with small insertion loss is realized. It is worthwhile to mention that the strong current distribution on two short dipoles at 7 GHz still agrees well with the discussions above.

The side view of electric-field distribution along the propagation direction of the incident wave is given in Fig. 8. We observed that at 3.6 GHz, the rasorber operates as a high-impedance surface absorber, there is almost no power leaking from the lossless FSS. The incident power is blocked on the lossy FSS layer and absorbed by the inserted lumped resistors of the lossy FSS. The power can penetrate the designed structure at 5.6 GHz, meanwhile the electric-field intensity in front of and beyond the rasorber are similar to each other. The strong resonance is introduced by the lossless layer rather than the lossy layer. It indicates that little power is consumed by the presented structure and a high transmittance window is achieved. At 7 GHz, the reflection becomes much stronger than that at 3.6 GHz and 5.6 GHz, and a little power is leaked by the structure at the same time. In other words, these phenomena match the analysis above, and the method can effectively provide a guideline to design a rasorber with a high transmittance window.

To validate the designed rasorber, an experimental prototype was fabricated with dimensions of 210 mm × 210 mm, and measured in an anechoic chamber. The pictures of the

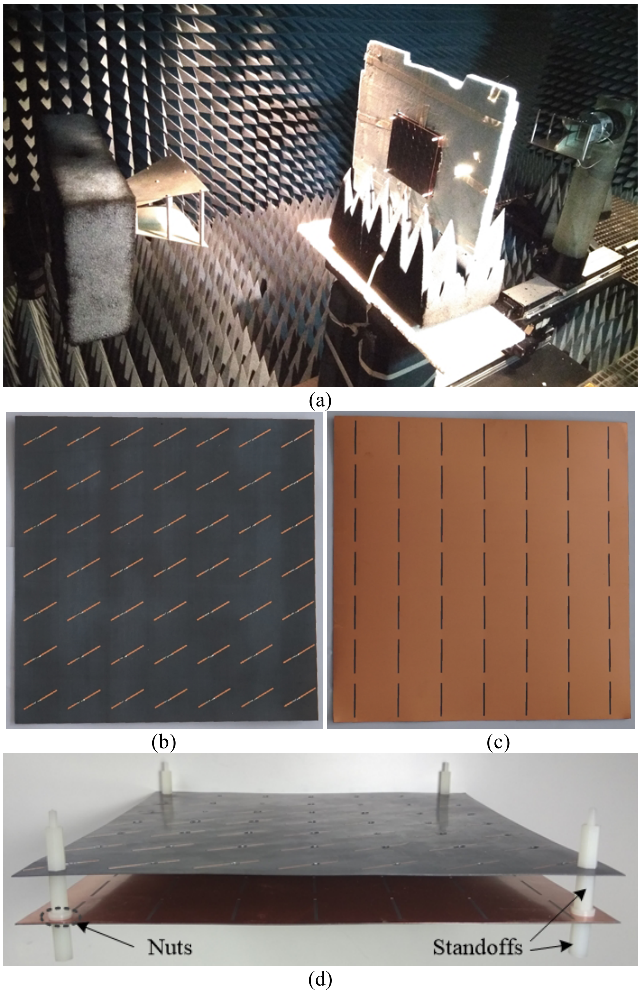

FIGURE 9. Photos of the fabricated rasorber. (a) Photo of the test setup. (b) Top view of the lossy FSS layer. (c) Top view of the lossless FSS layer. (d) Photo of the fabricated rasorber with the standoffs and nuts.

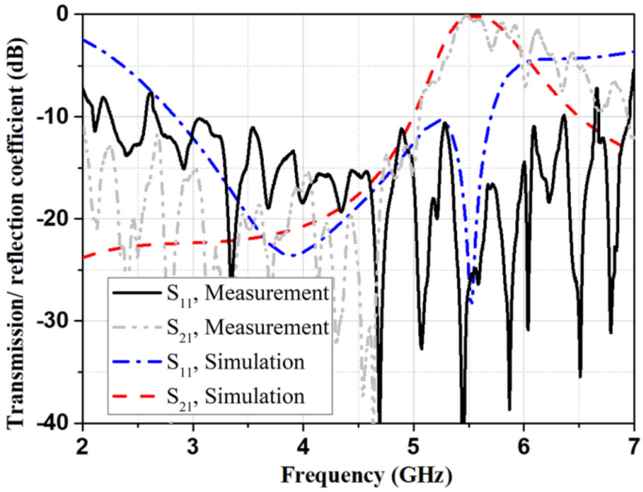

FIGURE 10. The comparison between simulation and measurement results.

TABLE 1. Performance comparison

Ref.	Maximum transmission and f_T	Absorption bandwidth, (-10 dB)	Strong reflection
[10]	-1.9 dB, 1 GHz, Sim.	8.4-19 GHz, (-20 dB)	yes
[11]	-0.3 dB, 4.6 GHz, Sim.	10-18 GHz, (-15 dB)	yes
[12]	-1 dB, 2 GHz, Mea.	4.5-12.5 GHz	yes
[13]	-1 dB, 1 GHz, Mea.	3-9 GHz	yes
[15]	-0.5 dB, 0.92 GHz, Mea.	3-9 GHz	yes
[17]	-1.2 dB, 21 GHz, Mea.	5-13 GHz	yes
[18]	-0.15 dB, 10.2 GHz, Mea.	3-9 GHz	yes
[19]	-0.3 dB, 10 GHz, Mea.	3.2-8.7 GHz	yes
[21]	-0.2 dB, 2.2 GHz, Mea.	0.92-1.43 GHz and 2.84-3.31 GHz, (-7 dB)	no
Our Work	-0.2 dB, 5.6 GHz, Mea.	2.8-5 GHz	no

Ref. = reference number, f_T = the frequency of maximum transmission coefficient, Mea. = measurement result, Sim. = simulation result, Strong reflection = strong reflection within the operation band.

fabricated prototype are shown in Fig. 9. The FSS structures are realized by printed circuit boards (PCB) technique, and both two layers are printed on the F4B substrate whose thickness and relative permittivity are 0.508 mm and 2.2, respectively. The plastic standoffs with a length of 15 mm are used to fix the lossy and lossless FSS layers. Meanwhile, the 0.5 mm thick plastic nuts are inserted between the lossy and lossless FSS layers to realize the air spacer with a thickness of 16 mm. The standoffs and nuts are located at the four corners of the rasorber to reduce the influence on the performance of the rasorber. The thickness of the F4B substrate is negligible compared to the thickness of the air spacer. The simulated and circuit calculation results show that the thin substrate has little effect on the performance of this design. The comparison between measured and simulated results is illustrated in Fig.10, showing that a transmission window is generated around 5.6 GHz and the reflection is controlled at a good level of lower than -10 dB during operation band. Several factors may result in discrepancies between the simulated and experimental results. Although the noise in the experimental system, fabrication errors and the influence of the welds have slightly shifted the resonance frequencies and introduced ripples into the results, the operation characteristics are verified.

To clearly demonstrate the performance of our design, a comparison is listed in terms of the maximum transmission and its frequency f_T, the -10 dB absorption bandwidth, and the strong reflection within operation band in Table I. It is worth to underline that some literatures use other criteria to describe the absorption bandwidth in [10], [11], and [21]. Through the relative relationship between the absorption band and f_T, it is seen that the absorption bands of many rasorber designs are located above the transmission frequencies. Meanwhile, strong reflection within the operation band is introduced in most designs, and the reflection reduction performance is influenced. The transmission band of our design locates at the frequencies above the absorption band with a comparatively small insertion loss. Moreover, the strong reflection between the absorption band and transmission band is reduced effectively, and a wide absorption band is realized.

V. CONCLUSION

A rasorber with a transmission window located at the upper frequencies of the absorption band has been presented in this paper. The dipole elements are used to realize the transmissive behavior, and the complex and costly structures are avoided. Meanwhile, the decoupling structure has been designed to achieve a relatively stable transmissive/absorptive performance. The current flowing across the two sides of the lumped resistor has been reduced by using crossed dipole elements. Therefore, the incident power is allowed to penetrate the presented rasorber with a low insertion loss. The wide absorption bandwidth has been realized with the presented rasorber, and the reflection between the absorption and transmission band is reduced to fulfill the wideband reflection reduction performance. The insertion loss is less than 1 dB under the oblique incidence up to 45°. Finally, the design has been fabricated, measured and validated.

REFERENCES

[1] S. M. Mahmood and T. A. Denidni, "A comparative study on switchable frequency-selective surfaces," *Microw. Opt. Technol. Lett.*, vol. 58, no. 4, pp. 839–844, Apr. 2016.

[2] L. Zhang, Q. Wu, and T. A. Denidni, "Electronically radiation pattern steerable antennas using active frequency selective surfaces," *IEEE Trans. Antennas Propag.*, vol. 61, no. 12, pp. 6000–6007, Dec. 2013.

[3] M. Z. Joozdani, M. K. Amirhosseini, and A. Abdolali, "Wideband RCS reduction of patch array antenna with miniaturized FSS," *Microw. Opt. Technol. Lett.*, vol. 58, no. 4, pp. 969–973, Apr. 2016.

[4] S. Genovesi, F. Costa, and A. Monorchio, "Wideband radar cross section reduction of slot antennas arrays," *IEEE Trans. Antennas Propag.*, vol. 62, no. 1, pp. 163–173, Jan. 2014.

[5] H. Zhou *et al.*, "Filter-antenna consisting of conical FSS radome and monopole antenna," *IEEE Trans. Antennas Propag.*, vol. 60, no. 6, pp. 3040–3045, Jun. 2012.

[6] Y. Han, W. Che, C. Christopoulos, Y. Xiong, and Y. Chang, "A fast and efficient design method for circuit analog absorbers consisting of resistive square-loop arrays," *IEEE Trans. Electromagn. Compat.*, vol. 58, no. 3, pp. 747–757, Jun. 2016.

[7] D.-U. Sim, J.-H. Kwon, Y.-J. Chong, and S.-O. Park, "Design of electromagnetic wave absorber using periodic structure and method to broaden its bandwidth based on equivalent circuit-based analysis," *IET Microw., Antennas Propag.*, vol. 9, no. 2, pp. 142–150, 2015.

[8] B.-K. Kim and B. Lee, "Wideband absorber at X-band adopting trumpet-shaped structures," *Electron. Lett.*, vol. 50, no. 25, pp. 1957–1959, 2014.

[9] F. Costa, A. Monorchio, and G. Manara, "Analysis and design of ultra thin electromagnetic absorbers comprising resistively loaded high impedance surfaces," *IEEE Trans. Antennas Propag.*, vol. 58, no. 5, pp. 1551–1558, May 2010.

[10] A. Motevasselian and B. L. G. Jonsson, "Design of a wideband rasorber with a polarisationsensitive transparent window," *IET Microw. Antennas Propag.*, vol. 6, no. 7, pp. 747–755, Mar. 2012.

[11] F. Costa and A. Monorchio, "A frequency selective radome with wideband absorbing properties," *IEEE Trans. Antennas Propag.*, vol. 60, no. 6, pp. 2740–2747, Jun. 2012.

[12] L. G. Liu and H. Cha, "Analysis and design of the invisible radome by LLumar glass," *J. Phys. D, Appl. Phys.*, vol. 47, no. 7, p. 075105, Jan. 2014.

[13] L. G. Liu *et al.*, "Design of an invisible radome by frequency selective surfaces loaded with lumped resistors," *Chin. Phys. Lett.*, vol. 30, no. 6, p. 064101, Dec. 2013.

[14] H. Zhou *et al.*, "Experimental demonstration of an absorptive/transmissive FSS with magnetic material," *IEEE Antennas Wireless Propag. Lett.*, vol. 13, pp. 114–117, 2014.

[15] Q. Chen, J. J. Bai, L. Chen, and Y. Q. Fu, "A miniaturized absorptive frequency selective surface," *IEEE Antennas Wireless Propag. Lett.*, vol. 14, pp. 80–83, 2015.

[16] X. Yuan and X. Yuan, "A transmissive/absorbing radome with double absorbing band," *Microw. Opt. Technol. Lett.*, vol. 58, no. 8, pp. 2016–2019, Aug. 2016.

[17] X. Chen, Y. Li, Y. Fu, and N. Yuan, "Design and analysis of lumped resistor loaded metamaterial absorber with transmission band," *Opt. Express*, vol. 20, no. 27, pp. 28347–28352, Dec. 2012.

[18] Q. Chen, L. Liu, L. Chen, J. Bai, and Y. Fu, "Absorptive frequency selective surface using parallel LC resonance," *Electron. Lett.*, vol. 52, no. 6, pp. 418–419, Mar. 2016.

[19] Q. Chen, S. Yang, J. Bai, and Y. Fu, "Design of absorptive/transmissive frequency-selective surface based on parallel resonance," *IEEE Trans. Antennas Propag.*, vol. 65, no. 9, pp. 4897–4902, Sep. 2017.

[20] Y. Shang, Z. Shen, and S. Xiao, "Frequency-selective rasorber based on square-loop and cross-dipole arrays," *IEEE Trans. Antennas Propag.*, vol. 62, no. 11, pp. 5581–5589, Nov. 2014.

[21] Z. Shen, J. Wang, and B. Li, "3-D frequency selective rasorber: Concept, analysis, and design," *IEEE Trans. Microw. Theory Techn.*, vol. 64, no. 10, pp. 3087–3096, Oct. 2016.

[22] B. Bian, S. Liu, and X. Kong, "Three-dimensional microwave broadband metamaterial absorber with broad transmission window based on the coupled symmetric split ring resonators," *J. Electromagn. Waves Appl.*, vol. 30, no. 16, pp. 2153–2164, Nov. 2016.

[23] J. Fu *et al.*, "Frequency-selective rasorber based on equivalent circuit analysis," presented at the ICEAA, 2017. [Online]. Available: https://ieeexplore.ieee.org/stamp/stamp.jsp?tp=&arnumber=8065668.

[24] D. M. Pozar, "Microwave network analysis," in *Microwave Engineering*, 3rd ed. Pittsburgh, PA, USA: Wiley, 2006, ch. 4, sec. 4, pp. 183–186.

[25] R. J. Langley and E. A. Parker, "Equivalent circuit model for arrays of square loops," *Electron. Lett.*, vol. 18, no. 7, pp. 294–296, Apr. 1982.

[26] F. Costa, A. Monorchio, and G. Manara, "Efficient analysis of frequency-selective surfaces by a simple equivalent-circuit model," *IEEE Antennas Propag. Mag.*, vol. 54, no. 4, pp. 35–48, Aug. 2012.

[27] N. Behdad and M. A. Al-Joumayly, "A generalized synthesis procedure for low-profile, frequency selective surfaces with odd-order bandpass responses," *IEEE Trans. Antennas Propag.*, vol. 58, no. 7, pp. 2460–2464, Jul. 2010.

[28] O. Luukkonen *et al.*, "Simple and accurate analytical model of planar grids and high-impedance surfaces comprising metal strips or patches," *IEEE Trans. Antennas Propag.*, vol. 56, no. 6, pp. 1624–1632, Jun. 2008.

ZHEFEI WANG was born in Harbin, China, in 1989. He received the M.S. degree in electronic of science and technology from the Harbin University of Science and Technology, China, in 2015. He is currently pursuing the Ph.D. degree in information and communication engineering with the Harbin Institute of Technology, China.

From 2018 to 2019, he was a Visiting Ph.D. Student at the Energy Materials Telecommunications Research Centre, Institut National de la Recherche Scientifique, Montreal, Canada. His research is focused on the analysis and modelling of the radar cross-section reduction system using frequency-selective surface, electromagnetic band gap, absorptive material, rasorber, and metamaterial.

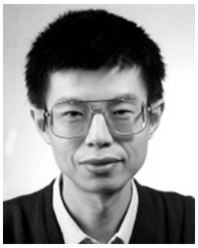

QINGSHENG ZENG (S'98–M'02–SM'11) received the Ph.D. degree from the University of Ottawa, Canada. He is currently a Distinguished Professor and the Ph.D. Advisor of the Nanjing University of Aeronautics and Astronautics, an Adjunct Professor and the Ph.D. Advisor of University of Ottawa, Carleton University, Université du Québec an Outaouais, and Institut National de la Recherche Scientifique–Centre Energie, Matériaux et Télécommunications, a Guest Professor of Harbin Engineering University, Northwestern Polytechnic University, Beijing University of Post and Telecommunications, and Beijing Jiaotong University. He has been a Research Engineer and a Senior Research Engineer at the Communications Research Centre Canada, Government of Canada. He has undertaken research and teaching in several fields, including antenna analysis and design, electromagnetic compatibility and interference (EMC/EMI), ultra-wideband technology, radio wave propagation, and computational electromagnetics. He has been a member of the Strategic Projects Grant Selection Panel (Information and Communications Technologies B) for the Natural Sciences and Engineering Research Council of Canada (NSERC), a member of the Site Visit Committee of NSERC Industrial Research Chair, and a reviewer of the NSERC Industrial R&D Fellowships. He is the Chair of Antennas and Propagation/Microwave Theory and Techniques Joint Chapter and Secretary of EMC Chapter of IEEE Ottawa, and a member of the IEEE Canada Industry Relations Committee.

He has published over 100 SCI and EI indexed papers and technical reports, authored one book and co-authored two book chapters, one of which has been downloaded over 3000 times only in one year after it was published in 2011. He received several technical and technical service awards, was ranked as one of the researchers at the Communications Research Centre Canada with the strongest impacts in 2011, and selected as a distinguished expert under the Plan of Hundreds of Talents of Shanxi Province in China in 2015 and an oversea prestigious advisor of Guangdong Province in 2017. He has been serving as an editorial board member and a reviewer for a number of technical books and scientific journals, as a conference co-chair, a session organizer and chair, a technical program committee member and reviewer, a short course/workshop/tutorial presenter, and a keynote speaker for many international and national symposia.

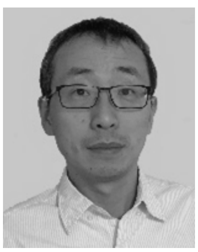

JIAHUI FU (SM'07) was born in Harbin, China, in 1973. He received the M.S. degree and the Ph.D. degree in information and communication engineering from the Harbin Institute of Technology in 1998 and 2005, respectively. He is currently a Professor with the School of Electronics and Information Engineering, Harbin Institute of Technology.

From 2009 to 2010, he was a Visiting Scholar in electrical engineering and computer science with The Pennsylvania State University. From 2017 to 2018, he was a Visiting Scholar in electrical and computer engineering with The University of British Columbia. His research interests include microwave and millimeter-wave circuits, antennas, metamaterials, and FSS.

He is currently a member of antenna branch of the China Electronic Society and IEEE Harbin AP Joint Chapter.

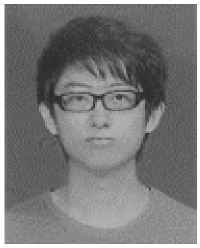

WAN CHEN received the B.S. degree in communication engineering, the M.S. degree in microwave engineering, and the Ph.D. degree in microwave engineering from the Harbin Institute of Technology, Harbin, China, in 2011, 2013, and 2017, respectively. He is currently a Post-Doctoral Researcher and a Research Associate in space environment simulation and research infrastructure with the Harbin Institute of Technology.

His research interests include the development of circular-polarized electric-scanning leaky-wave antenna based on composite right/left-handed transmission line, fundamental study of Autler-Townes splitting realized by all-dielectric materials, and wireless inter-chip connection by coupled relay.

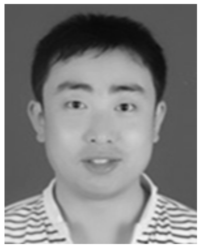

BO LV was born in Hegang, Heilongjiang, China, in 1984. He received the M.S. degree in circuit engineering from Xidian University, Nanchang, in 2007, and the Ph.D. degree in microwave engineering from HIT University, in 2018.

From 2010 to 2014, he was a Research Assistant with Junzhi Company, Xi'an, Shaanxi, China. His research interests include the development of metamaterial and plasma sources, fabrication of micro- or nanostructured surfaces.

MINGXIN SONG was born in Yichun, China, in 1974. He received the Diploma degree in electrical engineering from Jilin University in 1998, the M.S. degree in physics and chemistry of material in material science from the Harbin University of Science and Technology in 2005, and the Ph.D. degree in material Science from the Harbin University of Science and Technology in 2012. He is currently an Associate Professor with the School of Science, Harbin University of Science and Technology.

From 2008 to 2009, he was a Visiting Scholar in physical design methods of NXP semiconductors with The Netherlands. In 2014, he was a Visiting Scholar with the University of California, San Diego, CA, USA. His current research is focused on the new materials and the design of RF MEMS devices.

He is currently a Senior Member of the National Institute of Electromagnetism and the Heilongjiang Optical Association.

TAYEB A. DENIDNI (SM'09) received the M.Sc. and Ph.D. degrees in electrical engineering from Laval University, Quebec City, QC, Canada, in 1990 and 1994, respectively.

From 1994 to 2000, he was a Professor with the Engineering Department, Université du Quebec in Rimouski, Rimouski, QC, Canada, where he founded the Telecommunications Laboratory. Since 2000, he has been with the Institut National de la Recherche Scientifique (INRS), Université du Quebec, Montreal, QC, Canada. He found the RF Laboratory at INRS-EMT, Montreal. He has a great experience with antenna design and he is leading a large research group consisting of three research scientists, six Ph.D. students, and one M.Sc. student. He served as a Principal Investigator on many research projects sponsored by NSERC, FCI, and numerous industries. His current research areas of interests include reconfigurable antennas using EBG and FSS structures, dielectric resonator antennas, metamaterial antennas, adaptive arrays, switched multi-beam antenna arrays, ultra-wideband antennas, and microwave and development for wireless communications systems.

In 2012 and 2013, he received from INRS for outstanding research and teaching achievements. From 2005 to 2007, he has served as an Associate Editor for the IEEE ANTENNAS WIRELESS PROPAGATION LETTERS. From 2008 to 2010, he served as an Associate Editor for the IEEE TRANSACTIONS ON ANTENNAS PROPAGATION. Since 2015, he has served as an Associate Editor for *IET Electronics Letters*.